Slow electron velocity-map imaging spectroscopy of the C_4H^- and C_4D^- anions

Jia Zhou and Etienne Garand
Department of Chemistry, University of California, Berkeley, California 94720, USA

Daniel M. Neumark[a)]
Department of Chemistry, University of California, Berkeley, California 94720, USA and Chemical Sciences Division, Lawrence Berkeley National Laboratory, Berkeley, California 94720, USA

(Received 27 August 2007; accepted 17 September 2007; published online 19 October 2007)

High resolution photodetachment spectra of C_4H^- and C_4D^- obtained via slow electron velocity-map imaging (SEVI) are presented. The spectra reveal closely spaced transitions to the neutral $^2\Sigma^+$ and $^2\Pi$ states which can be distinguished based on the corresponding photoelectron angular distributions. The C_4H ground state is confirmed as the $\tilde{X}\,^2\Sigma^+$ state, with the excited $\tilde{A}\,^2\Pi$ state lying only 213 cm^{-1} higher (201 cm^{-1} for C_4D). The electron affinities (EAs) are slightly revised to EA $(C_4H)=28\,497\pm8$ cm^{-1} and EA $(C_4D)=28\,478\pm10$ cm^{-1}. Progressions in low frequency bending vibrations are observed in both states, yielding experimental frequencies of $\nu_7=179(169)$ cm^{-1} and $\nu_6=408(392)$ cm^{-1} for the $\tilde{X}\,^2\Sigma^+$ state of C_4H (C_4D), and $\nu_7=220(215)$ cm^{-1} and $\nu_6=446(437)$ cm^{-1} for the $\tilde{A}\,^2\Pi$ state. © *2007 American Institute of Physics*.
[DOI: 10.1063/1.2795723]

I. INTRODUCTION

The linear C_4H radical has received considerable attention in astronomy since its discovery in the envelope of a carbon star by radio astronomy in 1978;[1] it has since then been observed in numerous interstellar media.[2–7] The potential importance of C_4H as a precursor to polycyclic aromatic hydrocarbons in interstellar chemistry and combustion processes[8] has stimulated continued interest in this molecule. The C_4H and C_4D radicals have been studied in rare gas matrices with electron spin resonance[9] and Fourier-transform infrared spectroscopy,[10] and in the gas phase using millimeter and microwave,[11–14] laser-induced fluorescence (LIF),[15] and anion photoelectron (PE) spectroscopy.[16] The corresponding anion, C_4H^-, is also of interest as it is one of the few molecular negative ions identified in the interstellar medium[17] via its recently measured microwave spectrum.[18] In this paper, we probe the vibronic structure of the C_4H radical by slow electron velocity-map imaging (SEVI) of the anion.

The spectroscopy of the C_4H radical is particularly challenging owing to its close-lying $^2\Sigma^+$ and $^2\Pi$ states. In C_2H, the ground state is well established to be $^2\Sigma^+$, and the term energy of the $^2\Pi$ excited state is about 3700 cm^{-1}.[19–21] In C_6H, the order is reversed, with the $^2\Sigma^+$ excited state lying 1500 cm^{-1} above the $^2\Pi$ ground state.[16,22] This trend points to C_4H as the crossing point for the two electronic states. Experimental results[11,12,15] have indicated a $^2\Sigma^+$ ground state for C_4H, but electronic structure calculations[13,23–26] have shown that the $^2\Sigma^+$ and $^2\Pi$ states are nearly degenerate; the most recent work by Graf *et al.*[26] predicts that the $^2\Pi$ state lies only 35 meV above the $^2\Sigma^+$ state. On the experimental side, perturbed rotational lines in the millimeter wave spectra[3,12] and intensities of symmetry forbidden bands in LIF (Ref. 15) provide experimental evidence of vibronic interaction between the $^2\Sigma^+$ and $^2\Pi$ states. However, it has not been possible to determine the splitting between these two states directly using optical spectroscopy.

Photodetachment of C_4H^- provides another means of investigating the $^2\Sigma^+$ and $^2\Pi$ states. The anion is linear[18] with a $^1\Sigma^+$ ground state $(\cdots 1\pi^4 2\pi^4 9\sigma^2)$. Removal of an electron from the 9σ or 2π molecular orbital (MO) accesses the lowest lying $^2\Sigma^+$ or $^2\Pi$ neutral states, respectively, allowing both states to be probed on equal footing.

In the PE spectra of C_4H^- measured at 266 nm by Taylor *et al.*,[16] transitions to vibrational levels of both neutral states were partially resolved and identified by means of their differing photoelectron angular distributions (PADs), which were expected to be similar to the photodetachment of C_2H^- to the $^2\Sigma^+$ and $^2\Pi$ states of C_2H. The C_4H^- PE spectra were consistent with a $^2\Sigma^+$ ground state and a low-lying $^2\Pi$ state, but the origin of the $^2\Pi$ state was ambiguous owing to considerable spectral congestion. In a related experiment, Maier and co-workers[27,28] measured the electronic spectrum of C_4H^- in the vicinity of the detachment threshold, and found sharp autodetachment structure from excitation to a dipole-bound anion state based on the lowest lying $^2\Pi$ neutral core.

In this paper, we report photodetachment spectra of C_4H^- and C_4D^- using SEVI (Ref. 29) to shed more light on the two lowest electronic states of the C_4H radical. The SEVI technique was recently developed in our laboratory with the goal of attaining photodetachment spectra with sub-meV resolution while maintaining the ease of use and general applicability of PE spectroscopy. The SEVI spectra presented

a)Author to whom correspondence should be addressed. Electronic mail: dneumark@berkeley.edu

here focus on the region within 0.2 eV of the photodetachment threshold. Compared to the PE spectra, many new features are fully resolved and assigned. Distinctive PADs of the observed transitions aided in the assignment of the spectra.

II. EXPERIMENT

The SEVI apparatus has been described in detail elsewhere.[29–31] In SEVI, mass-selected anions are photodetached at selected wavelengths slightly above detachment threshold. The resulting photoelectrons are collected via velocity-map imaging[32] (VMI) using relatively low extraction voltages, with the goal of selectively detecting slow electrons with high efficiency and enlarging their image on the detector. A series of images can be obtained at different wavelengths, each yielding a high resolution photoelectron spectrum over a limited range of electron kinetic energy.

Briefly, C_4H^- (C_4D^-) anions were produced by expanding 250 psi of a mixture of 4% 1,2-butadiene (1,3-butadiene-d_4), 48% carbon dioxide, and 48% argon into the source vacuum chamber through an Even-Lavie pulsed valve[33] equipped with a circular ionizer. Anions formed in the gas expansion were perpendicularly extracted into a Wiley-McLaren time-of-flight mass spectrometer and directed to the detachment region by a series of electrostatic lens and pinholes. A 1 μs pulse on the last ion deflector allowed only ions of the desired mass into the interaction region. Anions were photodetached between the repeller and the extraction plates of the VMI electron optical assembly by the focused output of a Nd:YAG-pumped, tunable dye-laser (YAG denotes yttrium aluminum garnet). The photoelectron cloud formed was then coaxially extracted down a 50 cm flight tube and mapped onto a detector comprising a chevron-mounted pair of time-gated, imaging quality microchannel plates coupled to a phosphor screen, as is typically used in photofragment imaging experiments.[34] Events on the screen were collected by a 1024×1024 charge-coupled device camera and sent to a computer. Photoelectron velocity-mapped images resulting from 25 000–100 000 laser pulses were summed, quadrant symmetrized, and inverse-Abel transformed. Photoelectron spectrum was then obtained via angular integration of the transformed image.

The apparatus was calibrated by acquiring SEVI images of atomic chloride at several different photon energies for each repeller voltage used (150–350 V). In the 150 V images, the full width at half maximum (FWHM) was 1.7 cm^{-1} at 10 cm^{-1} above threshold, while in the 350 V images, the FWHM was 2.8 cm^{-1} at 23 cm^{-1} above threshold. Within a single image, all observed transitions have similar widths in pixels (Δr), which means that the transitions observed further from threshold (larger r) are broader in energy.

Overall, by varying the laser wavelength and VMI voltages, the instrument can be operated in distinct modes, as described previously,[35] offering high resolution over a small range of electron kinetic energy (eKE), or somewhat lower resolution over a broader eKE range. For example, the best resolution is obtained with low repeller voltages (to magnify the image) at photodetachment wavelengths close to a particular threshold. In any case, the spectra presented in the following section are taken under operating conditions yielding reasonable resolution and signal-to-noise ratio, taking into account that the ultimate linewidth in SEVI spectroscopy of molecular anions is generally determined by unresolved rotational structure rather than instrumental limitations.

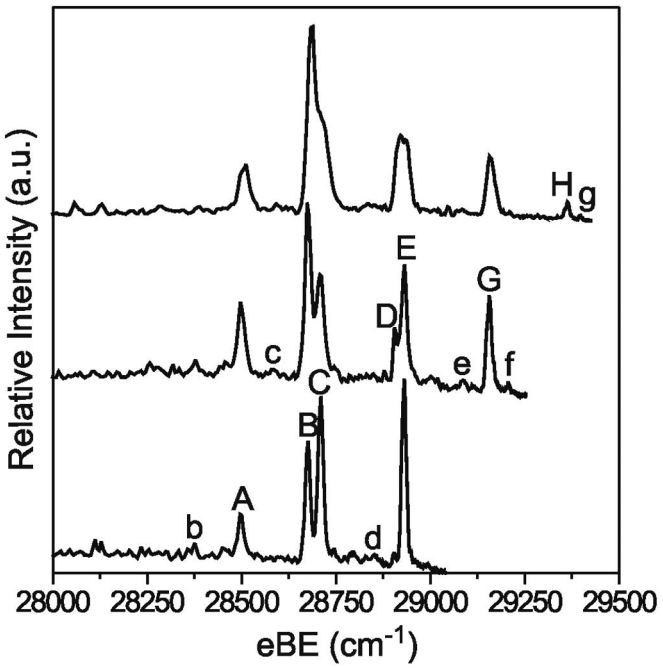

FIG. 1. SEVI spectra of C_4H^- taken at 150 V VMI voltage. The top trace was acquired with photon energy of 29 426.4 cm^{-1}; the middle trace was acquired with photon energy of 29 254.4 cm^{-1}; the bottom trace was acquired with photon energy of 29 042.2 cm^{-1}.

SEVI also provides information on the photoelectron angular distribution, given by[36]

$$\frac{d\sigma}{d\Omega} = \frac{\sigma_{\text{total}}}{4\pi}\left[1 + \beta(eKE)\left(\tfrac{3}{2}\cos^2(\theta) - \frac{1}{2}\right)\right], \quad (1)$$

for one-photon detachment, where θ is the angle between the direction of the photoelectron ejection and the polarization vector of the incident photon. The anisotropy parameter β lies between 2 and -1, corresponding to the $\cos^2\theta$ and $\sin^2\theta$ distributions, respectively. PADs provide information on the orbital angular momentum l of the ejected electron; s-wave ($l=0$) detachment leads to $\beta=0$, p-wave ($l=1$) to $\beta=2$, and $s+d$ wave to $\beta=-1$. In the case of C_4H, with its two lowest electronic states being almost degenerate, the PADs can be valuable in assigning transitions to the two states. While SEVI works best for s-wave detachment, we have recently shown[35] that it can yield comparable energy resolution when applied to p-wave processes.

III. RESULTS AND ANALYSIS

SEVI spectra of C_4H^- taken at repeller voltage of 150 V are presented in Fig. 1, while SEVI spectra of C_4D^- taken at 250 V are shown in Fig. 2. The spectra are plotted with respect to electron binding energy (eBE), the difference

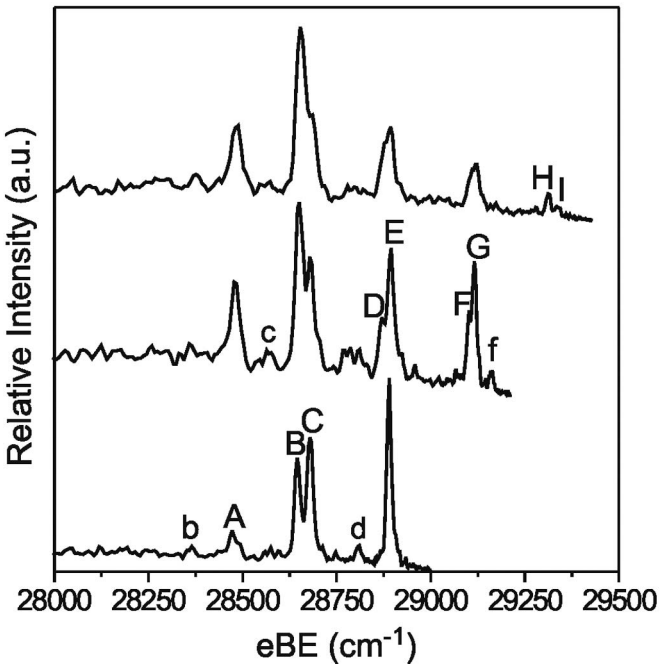

FIG. 2. SEVI spectra of C_4D^- taken at 250 V VMI voltage. The top trace was acquired with photon energy of 29 426.3 cm^{-1}; the middle trace was acquired with photon energy of 29 211.6 cm^{-1}; the bottom trace was acquired with photon energy of 29 000.0 cm^{-1}.

between the photon energy and the eKE,

$$\mathrm{eBE} = h\nu - \mathrm{eKE}. \tag{2}$$

The high energy termination point of each spectrum corresponds to the photon energy with which each image was acquired. The spectra presented in Figs. 1 and 2 are representative of the numerous images acquired with various photon energies during the experiment. The PE spectra from Ref. 16 are shown in Fig. 3, with the region corresponding to Figs. 1 and 2 shaded in gray.

The SEVI spectra of C_4H^- and C_4D^- in Figs. 1 and 2 are remarkably similar. Five well-separated bands are present in the same energy window for both isotopologues, corresponding to the partially resolved features in the previously recorded PE spectra. The higher resolution spectra in Figs. 1 and 2 reveal that several of the bands are doublets with splittings ranging from 15 to 35 cm^{-1}, and there are several additional minor peaks as well. The eBE of each feature is listed in Table I, and each peak is attributed to either *s*- or *p*-wave detachment, depending on its anisotropy parameter β. The markedly different PADs for the various features can be seen directly from the photoelectron image in Fig. 4, the SEVI image corresponding to the bottom spectrum in Fig. 1. The two rings corresponding to features B and C are clearly distinguished, and while C is isotropic, B is strongly peaked along the direction of laser polarization. Peaks F and G, the most closely spaced doublet, are resolved only in the C_4D^- SEVI spectrum.

The relative peak intensities change noticeably with photon energy. In particular, as the photon energy is lowered, the intensities of the *p*-wave scattering peaks A, B, and D drop compared to the *s*-wave peaks for both isotopologues. The dependence of peak intensities upon photon energy can be understood from the Wigner threshold law for anion photodetachment,[37]

$$\sigma \propto (\Delta E)^{l+0.5}, \tag{3}$$

where σ is the photodetachment cross section, and $\Delta E = (h\nu - E_{\mathrm{th}})$ is the difference between the photon energy and the detachment threshold. As a result, the cross section for *p*-wave detachment drops more rapidly close to threshold than that for *s*-wave detachment, consistent with our observations here and in previous work.[35] On this basis, although the PAD of peak F in Fig. 2 could not be accurately measured because this peak is only partially resolved, it is assigned to *s*-wave detachment because of its intensity in the middle trace, taken only 111 cm^{-1} above its detachment threshold. Similarly, several of the weak features observed close to their detachment thresholds most likely scatter via *s*-wave.

IV. DISCUSSION

Table I shows that, of the main features in the SEVI spectra, peaks A, B, and D are associated with *p*-wave scattering, while peaks C, E, F, G, and H are from *s*-wave scattering. These results imply that the two groups of peaks correspond to photodetachment transitions to two different electronic states of C_4H. Prior work[16,35,38] on C_2H^- showed that detachment from the highest occupied σ or π MOs generates the $\tilde{X}\,^2\Sigma^+$ or $\tilde{A}\,^2\Pi$ state of C_2H, proceeding via *p*- or *s*-wave scattering, respectively. Correspondingly, the C_4H SEVI results point to assigning peaks A, B, and D to detachment to the $^2\Sigma^+$ state and the remaining major peaks to the $^2\Pi$ state. Using this assignment, we will show that all the major features in the SEVI spectra can be assigned. However, the attribution of each peak to a single electronic state is somewhat of a simplification given that significant vibronic coupling between the two C_4H states is expected; the resultant effects are discussed at the end of this section.

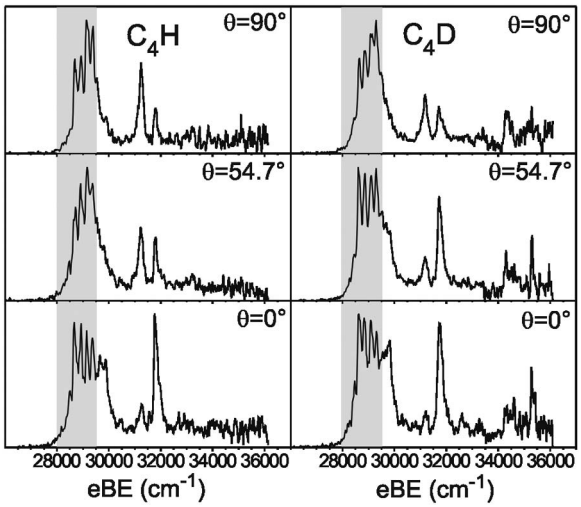

FIG. 3. PE spectra of C_4H^- and C_4D^- adapted from Ref. 16. Laser polarization angles are indicated. The gray shaded areas indicate the regions covered by the SEVI spectra in Figs. 1 and 2.

TABLE I. Peak positions (cm^{-1}) and PADs for the features observed in the C_4H^- and C_4D^- SEVI spectra. The uncertainties in the eBE values are ± 10 cm^{-1} for most transitions; ± 25 cm^{-1} for those marked with *. The PADs are listed as "*s*" for *s*-wave detachment with $\beta \cong 0$ and "*p*" for *p*-wave detachment with $\beta \cong 2$; several of the weak peaks have uncertain PADs and are, thus, left blank.

Peak	C_4H eBE (cm^{-1})	Splitting from A (cm^{-1})	C_4D eBE (cm^{-1})	Splitting from A (cm^{-1})	PAD
b	28 380*	−117	28 370*	−108	
A	28 497	0	28 478	0	*p*
c	28 585*	88	28 561*	83	
B	28 676	179	28 647	169	*p*
C	28 710	213	28 679	201	*s*
d	28 830*	333	28 810*	332	
D	28 905	408	28 870	392	*p*
E	28 930	433	28 894	416	*s*
e	29 085*	588			
F			29 100	622	*s*
G	29 156	659	29 116	638	*s*
f	29 209	710	29 161	683	*s*
H	29 363	866	29 812	834	*s*
I			29 337	859	*s*
g	29 397	900			*s*

Peaks A and C are the first major features exhibiting *p*- and *s*-wave detachment, and are therefore assigned as the vibrational origins of the $^2\Sigma^+$ and $^2\Pi$ states. Peak A corresponds to a partially resolved feature in the earlier PE spectrum[16] which had been assigned to a hot band transition. However, upon examination of the traces in both Figs. 1 and 2, the high intensity of peak A compared to any features at lower eBE (i.e., peak b) strongly support its assignment as the origin transition.

These assignments of peaks A and C fix the $^2\Sigma^+$ state of C_4H as the ground state, in agreement with previous experiments,[11,12,15] and yield a splitting of only 213 cm^{-1} (26 meV) between the $\tilde{X}\,^2\Sigma^+$ and $\tilde{A}\,^2\Pi$ states. This splitting is quite close to the value of 35 meV recently reported in a high level electronic structure calculation by Graf *et al.*[26] Moreover, our assignment of peak A yields new values for the electron affinities of C_4H and C_4D: $28\,497 \pm 8$ cm^{-1} (3.5332 ± 0.0010 eV) and $28\,478 \pm 10$ cm^{-1} (3.5308 ± 0.0011 eV), respectively.

Some of the vibrational structure in the SEVI spectra can be assigned by comparison with electronic structure calculations; the work by Graf *et al.*[26] is particularly useful in this regard. C_4H has seven vibrational modes: four stretching modes (ν_{1-4}) with σ symmetry, and three degenerate bending modes (ν_{5-7}) with π symmetry. Graf *et al.*[26] calculated that the bending frequencies are all lower than the stretch frequencies for both the $\tilde{X}\,^2\Sigma^+$ and $\tilde{A}\,^2\Pi$ states of C_4H. The calculated frequencies for the ν_4 mode, the lowest frequency stretch, are 924 and 907 cm^{-1}, respectively, for the $\tilde{X}$ and $\tilde{A}$ states. Inspection of Table I shows that the peak spacings in the SEVI spectra are considerably less than these values, indicating that we are primarily observing progressions in the bending modes of both states. Assignments for both states and calculated frequencies of the two isotopologues are listed in Table II.

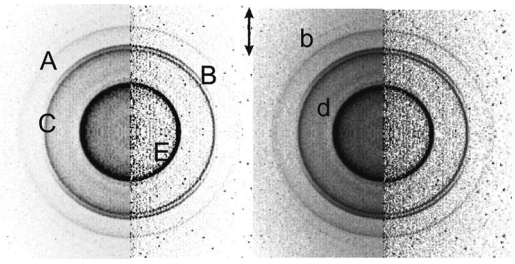

FIG. 4. SEVI image of C_4H^- taken at 29 042.2 cm^{-1} with 150 V VMI, corresponding to the bottom SEVI spectrum in Fig. 1. The left composite image consists of linear intensity plots of the symmetrized raw and transformed images, showing peaks A, B, C, and E, labeled accordingly. The right composite image consists of log intensity plots, showing the faint rings corresponding to the very weak peaks b and d, labeled accordingly.

We first consider the $\tilde{X}\,^2\Sigma^+$ state. Peaks B and D lie 179 and 408 cm^{-1} from peak A, the band origin. They are assigned to the $\tilde{X}7_0^1$ and $\tilde{X}6_0^1$ transitions, by comparison to the calculated harmonic frequencies of 178.3 and 379.3 cm^{-1} for the ν_7 and ν_6 modes. Deuteration results in small shifts of 10 and 16 cm^{-1} for peaks B and D, consistent with the vibrational analysis by Graf *et al.*[26] showing that both modes primarily involve bending motion of the carbon atoms. No progressions in ν_5, the CCH bending mode, with a calculated frequency of 578.4 cm^{-1},[26] are observed in the SEVI spectra.

Peak spacings within the $\tilde{A}\,^2\Pi$ state are comparable to those in the $\tilde{X}\,^2\Sigma^+$ state, again implying dominant activity in the low frequency bending modes. Comparison with theory is not as straightforward in the excited state since Renner-Teller (RT) effects can cause an unphysical splitting in the calculated harmonic frequencies for the degenerate bending modes, particularly when vibronic coupling between electronic states is also present.[39] In the case of the ν_7 mode, the calculated harmonic frequencies are 276.2 and 207.3 cm^{-1} for the a' and a'' components, respectively.[26] Given the relatively small splitting, the averaged value of 240 cm^{-1} should have some physical validity and, in fact, is close to the separation between peaks C and E. We then assign peak E in the

TABLE II. Assignment for the major observed transitions in the C_4H^- and C_4D^- SEVI spectra. All values are in cm^{-1}.

Assignment	C_4H peak	Splitting from $\tilde{X}0_0^0$	Splitting from $\tilde{A}0_0^0$	*Ab initio* freq.[a]	C_4D peak	Splitting from $\tilde{X}0_0^0$	Splitting from $\tilde{A}0_0^0$	H/D shift
$\tilde{X}0_0^0$	A	0			A	0		19
$\tilde{X}7_0^1$	B	179		178.3	B	169		10
$\tilde{A}0_0^0$	C		0		C		0	31
$\tilde{X}6_0^1$	D	408		379.3	D	392		16
$\tilde{A}7_0^1$	E		220		E		215	5
$\tilde{A}7_0^2$	F		446		F		421	25
$\tilde{A}6_0^1$	G		446		G		437	9
$\tilde{A}7_0^3$	H		653		H		633	20
$\tilde{A}6_0^1 7_0^1$					I		658	

[a]The *ab initio* frequencies for C_4H are from Ref. 26.

C_4H^- SEVI spectrum to the $\tilde{A}7_0^1$ transition, yielding a vibrational frequency of 220 cm^{-1} for the ν_7 mode on the $\tilde{A}\,^2\Pi$ state; the corresponding assignment of peak E in the C_4D^- spectrum yields a frequency of 215 cm^{-1}, again a very small isotope shift consistent with C–C bending. It is well known that RT effects induce splittings in the bending vibrational levels of linear molecules, with singly excited levels of $^2\Pi$ states splitting into three sublevels.[40] However, as discussed below, we expect transitions from the anion ground state to only one of these sublevels (i.e., for $\nu_7=1$, the vibronic level with Σ^+ symmetry) to occur in the SEVI spectrum.

Comparison with calculations for the ν_6 mode is less straightforward. Graf *et al.*[26] found widely divergent harmonic frequencies of 447.3 and 2007.3 cm^{-1} for the a'' and a' components of this mode and attributed the very large a' value to vibronic coupling with the $^2\Sigma^+$ state. The lower frequency component was found to be less sensitive and should be considerably closer to the SEVI experimental value. Based on these considerations, we assign the closely spaced doublet F and G in the C_4D^- spectrum to the $\tilde{A}7_0^2$ and $\tilde{A}6_0^1$ transitions, respectively, although this assignment could certainly be reversed. The single peak G in C_4H^- spectrum is assigned to the same two transitions which are overlapped in this case. Our assignment of peak G yields ν_6 fundamentals of 446 and 437 cm^{-1} for C_4H and C_4D, respectively. Peak H in the SEVI spectra of the two isotopologues is assigned to the $\tilde{A}7_0^3$ transition. The relatively weak peak I, at 658 cm^{-1} above $\tilde{A}$ state origin in C_4D, is assigned to the $\tilde{A}6_0^1 7_0^1$ combination band.

There are several other weak transitions observed in the C_4H^- and C_4D^- spectra, labeled with lower case letters and listed in Table I. In Figs. 1 and 2, some of these features are not obvious from the baseline, but their presence is clearer in the images, and they are also observed in other experimental spectra not shown here, taken at various photon energies. For example, the small peaks b and d, while barely distinguishable from the baseline in Fig. 1, appears as faint rings in Fig. 4. These peaks are likely to be transitions from vibrationally hot anion to vibrational levels of the $\tilde{X}\,^2\Sigma^+$ and $\tilde{A}\,^2\Pi$ states. Peaks b, c, and d lie 330, 345, and 326 cm^{-1} below peaks C, E, and G, respectively, in the C_4H^- spectra, with analogous splittings of 309, 333, and 306 cm^{-1} in the C_4D spectra. This suggests that they are transitions to the $\nu=0$, $\nu_7=1$, and $\nu_6=1$ levels of the $\tilde{A}\,^2\Pi$ state originating from a vibrationally excited anion state with frequencies of around 330 cm^{-1} in C_4H^- and 310 cm^{-1} in C_4D^-. This is reasonable considering that peaks C, E, and G are among the strongest transitions observed. However, the actual assignment of this anion level is somewhat ambiguous. Its frequency falls between the calculated anion vibrational frequencies[41] of $\nu_7=206$ cm^{-1} and $\nu_6=412$ cm^{-1}. Pino *et al.*[27] observed weak hot band transitions in the electronic spectrum of C_4H^- and C_4D^- lying 309.5 and 266 cm^{-1}, respectively, below the origin. These spacings are similar but slightly smaller than ours, and were assigned as 6_1^0 hot band transitions to the $K=2$ rotational level of a nonlinear anion excited state, discussed in more detail below.

It is of interest to compare our SEVI spectra with the gas phase electronic spectra of C_4H^- measured by Maier and co-workers.[27,28] In those experiments, sharp autodetachment structure was observed and assigned to excitation to the $^1A'$ state of the anion, located very close to the detachment threshold. They observed a vibrational progression of four peaks spaced by about 230 cm^{-1}, and the origin peak was rotationally resolved. The $^1A'$ state was attributed to a dipole-bound state with the neutral core having the same MO configuration as the $\tilde{A}\,^2\Pi$ state of the C_4H radical, since this state is calculated to have a significantly higher dipole moment than the $\tilde{X}\,^2\Sigma^+$ state (5 versus 0.8 D).[13,24] The vibrational progression was assigned to the ν_7 mode of the $^1A'$ state. Hence, we observe a remarkable degree of consistency between Maier and co-workers' work and ours, since the primary progression we observe in photodetachment to the $\tilde{A}\,^2\Pi$ state is also in the ν_7 mode with approximately the same frequency and relative intensity. This overall agreement supports the assignments of the progressions in the two sets of experiments, because a dipole-bound anion state should be quite similar to its parent neutral state. We point out, however, that rotational analysis[28] suggests a slightly bent geometry for the $^1A'$ state, in contrast to the linear structure cal-

culated for the neutral $\tilde{A}\,^2\Pi$ state. Note that, to our knowledge, no experimental evidence has been reported that directly supports the linearity of the $\tilde{A}\,^2\Pi$ state.

Our analysis of the vibrational structure in the SEVI spectra has resulted in a small downward revision of electron affinity EA(C_4H), from 3.558(15) eV, obtained via photoelectron spectroscopy,[16] to 3.5332(10) eV. This new value requires a minor reinterpretation of the electronic autodetachment spectrum. The vibrational origin of the band found by Maier and co-workers[27,28] at 28 674 cm^{-1} (3.555 eV) is below the original EA, so it was attributed to a bound level of the excited anion state with respect to electron detachment. Indeed, the enhanced intensity when two-color photodetachment technique was applied suggested a bound state. Our new results show that this anion state lies above the neutral $\tilde{X}\,^2\Sigma^+$ state but below the vibrational origin of the $\tilde{A}\,^2\Pi$ state at 28 710 cm^{-1}. This means that the vibrational ground state of the anion $^1A'$ state can autodetach to the $\tilde{X}\,^2\Sigma^+$ state, but only via electronic autodetachment involving a transition from the 9σ to 2π MOs of the neutral core. In contrast, the higher members of the progression lie above the $\tilde{A}\,^2\Pi$ state origin and can decay via vibrational autodetachment.

We close with further comments about the SEVI spectra. The assignments of the main features to bending progressions in the two neutral electronic states seem reasonable considering the low frequencies involved. However, the presence, let alone the dominance, of activity in the bending modes is unusual considering that the anion and both neutral states are believed to be linear. In a strict Franck-Condon picture, odd $\Delta\nu$ transitions in non-totally symmetric vibrations such as bending modes in linear molecules are forbidden, and even $\Delta\nu$ transitions (other than $\Delta\nu=0$) are very weak unless there is a substantial change in frequency upon photodetachment. Hence, we must consider the possible effects of vibronic coupling on our spectra.

There are two effects to consider here: RT coupling within the $\tilde{A}\,^2\Pi$ state, and Herzberg-Teller (HT) coupling between the $\tilde{X}\,^2\Sigma^+$ and $\tilde{A}\,^2\Pi$ states.[40] RT coupling splits excited levels of the degenerate bending modes in Π electronic states, so that, for example, the $\nu_7=1$ level of the $\tilde{A}\,^2\Pi$ state, for which the vibrational wavefunction has Π symmetry, is split into three vibronic levels with Σ^+, Σ^-, and Δ symmetries. However, the resulting states are linear combinations of vibrational wavefunctions with total vibrational angular momentum $l=\pm1$, so RT coupling alone will not allow transitions to these levels from the anion vibrational ground state. Hence, we must consider the additional effects from HT coupling.

Herzberg-Teller coupling mixes close-lying levels of the same vibronic symmetry that are nominally associated with different electronic states. Thus, odd levels of bend modes of the $\tilde{X}\,^2\Sigma^+$ state, with overall Π vibronic symmetry, can mix with even levels of bend modes of the $\tilde{A}\,^2\Pi$ state with the same vibronic symmetry, and transitions from the anion ground state to these levels become allowed. Similarly, odd bending levels of the $\tilde{A}\,^2\Pi$ state with Σ^+ symmetry mix with Σ^+ levels of the $\tilde{X}\,^2\Sigma^+$ state and become accessible to detachment from the anion ground state. These effects are well documented in C_2H,[20,21,42] where the $\tilde{X}\,^2\Sigma^+$ and $\tilde{A}\,^2\Pi$ states are separated by about 3700 cm^{-1}, and should be even stronger in C_4H where the separation is more than a factor of 10 less. Indeed, two prior spectroscopic studies of C_4H have demonstrated strong HT coupling between the two states. Yamamoto *et al.*,[12] using microwave spectroscopy, observed spin-orbit splittings around 3 cm^{-1} for excited bending levels of the $\tilde{X}\,^2\Sigma^+$ state, a clear indication of mixing with close-lying levels of the $\tilde{A}\,^2\Pi$ state. Hoshina *et al.*[15] investigated the $\tilde{B}\,^2\Pi$-$\tilde{X}\,^2\Sigma^+$ transition using LIF, finding strong transitions to odd bending levels of the upper state with Σ^+ vibronic symmetry that could only be explained by invoking strong HT coupling between the $\tilde{X}\,^2\Sigma^+$ and $\tilde{A}\,^2\Pi$ states.

Our SEVI spectra, which show strong odd $\Delta\nu$ transitions in the bending modes of both the $\tilde{X}\,^2\Sigma^+$ and $\tilde{A}\,^2\Pi$ states, can be explained within the context of HT coupling with additional contributions from RT coupling. There is, however, one aspect of our results that does not quite fit into this picture. In previous work, we and others have observed that when a transition in photodetachment becomes allowed through HT coupling, its PAD is characteristic of the electronic state from which the intensity is borrowed.[35,38,43] We would, for example, expect transitions to odd bend levels of the $\tilde{X}\,^2\Sigma^+$ state to proceed via *s*-wave detachment. We do not observe this; all transitions assigned to the $\tilde{X}\,^2\Sigma^+$ state appear to be *p*-wave, while all those to the $\tilde{A}\,^2\Pi$ state are *s*-wave. Hence, HT coupling appears to explain the presence of bend progressions in the SEVI spectra but not the pattern of PADs.

There is one additional aspect of C_4H^- photodetachment that may be playing a role here. The photodetachment cross section measured by Pino *et al.*[27] shows autodetachment peaks, as discussed above, superimposed on a rising background from direct detachment. However, these features are fairly broad, and photodetachment of the anion anywhere near threshold (as is required in SEVI) is likely to have a nonzero component from autodetachment. Since the autodetaching anion state is bent,[28] it is possible that the simple Franck-Condon picture of direct detachment to the radical is inadequate to describe either the photoelectron intensity or photoelectron angular distribution near the detachment threshold. For example, autodetachment through a bent excited state can populate bend-excited levels of C_4H even in the absence of HT coupling between the two neutral states, and the combined effects of autodetachment and HT coupling on the PAD are not well understood. While we remain confident of our assignments of the major peaks in the SEVI spectra of the $\tilde{X}\,^2\Sigma^+$ and $\tilde{A}\,^2\Pi$ states, it is clear the photodetachment of C_4H^- is unusually complex and requires further consideration.

V. CONCLUSIONS

SEVI spectra of the C_4H^- and C_4D^- anions are reported, resolving features associated with photodetachment to the $\tilde{X}\,^2\Sigma^+$ and $\tilde{A}\,^2\Pi$ states of the radical, many of which were not

previously observed. It was found that the $\tilde{X}\,^2\Sigma^+$ and $\tilde{A}\,^2\Pi$ states are only separated by 213 cm^{-1} in C_4H (201 cm^{-1} in C_4D). Low frequency bending vibrations were also observed on both states, giving the experimental frequencies of $\nu_7 = 179(169)$ cm^{-1} and $\nu_6 = 408(392)$ cm^{-1} on the $\tilde{X}$ state, and $\nu_7 = 220(215)$ cm^{-1} and $\nu_6 = 446(437)$ cm^{-1} on the $\tilde{A}$ state of the C_4H (C_4D) radical. Anomalies involving the intensities of the vibrational transitions and their PADs point to vibronic coupling between the two neutral states, and possibly to detachment mediated by an excited electronic state of the anion.

ACKNOWLEDGMENTS

This research is supported by the National Science Foundation under Grant No. DMR-0139064. E.G. thanks the Natural Science and Engineering Research Council of Canada for a postgraduate scholarship.

[1] M. Guelin, S. Green, and P. Thaddeus, Astrophys. J. **224**, L27 (1978).
[2] B. E. Turner, Astrophys. J. **347**, L39 (1989).
[3] M. Guelin, J. Cernicharo, S. Navarro, D. R. Woodward, C. A. Gottlieb, and P. Thaddeus, Astron. Astrophys. **182**, L37 (1987).
[4] M. B. Bell, P. A. Feldman, and H. E. Matthews, Astrophys. J. **273**, L35 (1983).
[5] M. B. Bell, T. J. Sears, and H. E. Matthews, Astrophys. J. **255**, L75 (1982).
[6] W. M. Irvine, B. Hoglund, P. Friberg, J. Askne, and J. Ellder, Astrophys. J. **248**, L113 (1981).
[7] S. E. Cummins, M. Morris, and P. Thaddeus, Astrophys. J. **235**, 886 (1980).
[8] J. H. Kiefer, S. S. Sidhu, R. D. Kern, K. Xie, H. Chen, and L. B. Harding, Combust. Sci. Technol. **82**, 101 (1992).
[9] K. I. Dismuke, W. R. M. Graham, and W. Weltner, J. Mol. Spectrosc. **57**, 127 (1975).
[10] L. N. Shen, T. J. Doyle, and W. R. M. Graham, J. Chem. Phys. **93**, 1597 (1990).
[11] C. A. Gottlieb, E. W. Gottlieb, P. Thaddeus, and H. Kawamura, Astrophys. J. **275**, 916 (1983).
[12] S. Yamamoto, S. Saito, M. Guelin, J. Cernicharo, H. Suzuki, and M. Ohishi, Astrophys. J. **323**, L149 (1987).
[13] M. C. McCarthy, C. A. Gottlieb, P. Thaddeus, M. Horn, and P. Botschwina, J. Chem. Phys. **103**, 7820 (1995).
[14] W. Chen, S. E. Novick, M. C. McCarthy, C. A. Gottlieb, and P. Thaddeus, J. Chem. Phys. **103**, 7828 (1995).
[15] K. Hoshina, H. Kohguchi, Y. Ohshima, and Y. Endo, J. Chem. Phys. **108**, 3465 (1998).
[16] T. R. Taylor, C. S. Xu, and D. M. Neumark, J. Chem. Phys. **108**, 10018 (1998).
[17] J. Cernicharo, M. Guelin, M. Agundez, K. Kawaguchi, M. C. McCarthy, and P. Thaddeus, Astron. Astrophys. **467**, L37 (2007).
[18] H. Gupta, S. Brunken, F. Tamassia, C. A. Gottlieb, M. C. McCarthy, and P. Thaddeus, Astrophys. J. **655**, L57 (2007).
[19] R. F. Curl, P. G. Carrick, and A. J. Merer, J. Chem. Phys. **82**, 3479 (1985).
[20] R. Tarroni and S. Carter, J. Chem. Phys. **119**, 12878 (2003).
[21] W. B. Yan, C. B. Dane, D. Zeitz, J. L. Hall, and R. F. Curl, J. Mol. Spectrosc. **123**, 486 (1987).
[22] H. Linnartz, T. Motylewski, O. Vaizert, J. P. Maier, A. J. Apponi, M. C. McCarthy, C. A. Gottlieb, and P. Thaddeus, J. Mol. Spectrosc. **197**, 1 (1999).
[23] M. Kolbuszewski, Astrophys. J. **432**, L63 (1994).
[24] D. E. Woon, Chem. Phys. Lett. **244**, 45 (1995).
[25] A. L. Sobolewski and L. Adamowicz, J. Chem. Phys. **102**, 394 (1995).
[26] S. Graf, J. Geiss, and S. Leutwyler, J. Chem. Phys. **114**, 4542 (2001).
[27] T. Pino, M. Tulej, F. Guthe, M. Pachkov, and J. P. Maier, J. Chem. Phys. **116**, 6126 (2002).
[28] M. Pachkov, T. Pino, M. Tulej, F. Guethe, K. Tikhomirov, and J. P. Maier, Mol. Phys. **101**, 583 (2003).
[29] A. Osterwalder, M. J. Nee, J. Zhou, and D. M. Neumark, J. Chem. Phys. **121**, 6317 (2004).
[30] M. J. Nee, A. Osterwalder, J. Zhou, and D. M. Neumark, J. Chem. Phys. **125**, 014306 (2006).
[31] J. Zhou, E. Garand, W. Eisfeld, and D. M. Neumark, J. Chem. Phys. **127**, 034304 (2007).
[32] A. T. J. B. Eppink and D. H. Parker, Rev. Sci. Instrum. **68**, 3477 (1997).
[33] U. Even, J. Jortner, D. Noy, N. Lavie, and C. Cossart-Magos, J. Chem. Phys. **112**, 8068 (2000).
[34] D. W. Chandler and P. L. Houston, J. Chem. Phys. **87**, 1445 (1987).
[35] J. Zhou, E. Garand, and D. M. Neumark, J. Chem. Phys. **127**, 114313 (2007).
[36] J. Cooper and R. N. Zare, J. Chem. Phys. **48**, 942 (1968).
[37] E. P. Wigner, Phys. Rev. **73**, 1002 (1948).
[38] K. M. Ervin and W. C. Lineberger, J. Phys. Chem. **95**, 1167 (1991).
[39] J. F. Stanton, J. Chem. Phys. **115**, 10382 (2001).
[40] G. Herzberg, *Electronic Spectra and Electronic Structure of Polyatomic Molecules* (Van Nostrand, New York, 1996).
[41] P. Botschwina, S. Seeger, M. Mladenovic, B. Schulz, M. Horn, S. Schmatz, J. Flugge, and R. Oswald, Int. Rev. Phys. Chem. **14**, 169 (1995).
[42] M. Peric, R. J. Buenker, and S. D. Peyerimhoff, Mol. Phys. **71**, 673 (1990).
[43] K. R. Asmis, T. R. Taylor, and D. M. Neumark, J. Chem. Phys. **111**, 8838 (1999).